JOURNAL OF APPLIED PHYSICS VOLUME 91, NUMBER 10 15 MAY 2002

Character of defects at an ion-irradiated buried thin-film interface

R. Kalyanaraman[a)]
Oak Ridge National Laboratory, Oak Ridge, Tennessee 37831;
Agere System, 700 Mountain Avenue, Murray Hill, New Jersey 07974;
and Department of Physics, Washington University, St. Louis, Missouri 63130

T. E. Haynes and O. W. Holland
Oak Ridge National Laboratory, Oak Ridge, Tennessee 37831

G. H. Gilmer[b)]
Agere System, 700 Mountain Avenue, Murray Hill, New Jersey 07974

(Received 1 October 2001; accepted for publication 25 February 2002)

In order to investigate the nature of defects produced by ion irradiation through a heterostructure, a silicon-on-insulator substrate with a buried SiO_2 layer at a depth of $\sim 1.5\ \mu m$ was irradiated. The implantation was done using 2 MeV $^{28}Si^+$ ions in the dose range of $0.2-1\times10^{16}\ cm^{-2}$. The subsequent defect analysis was performed using the Au labeling technique. Besides the presence of an expected excess of vacancy-type defects in the Si overlayer (V_{Si}^{ex}), an additional vacancy excess peak was observed at the frontside of the buried interface (V_{Int}^{ex}). The V_{Int}^{ex} is found to increase linearly with increasing dose of the high-energy implant. The presence of this V_{Int}^{ex} peak near the interface is also predicted by the TRIM Monte Carlo code. Additional Monte Carlo simulations of damage production via high-energy implantation in Si/X-type structures show that the nature of the defects at the front Si/X interface can be changed from vacancy to interstitial-type by increasing the mass of atoms in the buried thin-film, X. These experiments provide quantitative verification of nonuniform defect production at an ion-irradiated buried interface in Si. © *2002 American Institute of Physics.* [DOI: 10.1063/1.1470258]

I. INTRODUCTION

In recent times, the idea of integrating different materials with Si and other substrates has grown in importance due to the tremendous potential to make sophisticated devices. The integrated materials approach can lead to structures with opto-, electro-, and mechanical abilities coupled onto a single chip.[1] This obviously attractive possibility brings with it a number of processing complications, among which thermal expansion mismatch[2] and the presence of the numerous interfaces are particularly important. The presence of thermal expansion mismatches will be manifest in any thermal treatments of the integrated structures, while the interfaces will appear in the coupling of properties between the various layers.

In this view, postprocessing of the structures to control strain and interface properties will require techniques that are capable of a spatial deposition of energy as well as mass. Ion implantation is the primary technique for such situations. It can be used to modify bulk as well as interfacial properties, via doping, intermixing, etc. In fact, one of the most extensively studied problems is that of radiation-induced mixing across interfaces. Numerous books[3] and review articles[4] are available on the topic of ion-beam mixing of interfaces and buried thin films. However, these studies have typically relied on the detection of interfacial intermixing via spectrometric techniques like Rutherford backscattering (RBS) or secondary ion mass spectrometry (SIMS). The direct quantitative detection of interstitials and vacancies has been difficult. Numerous techniques have been used to profile point defects following implantation. For example, positron annihilation spectroscopy,[5] ion channeling,[6] impurity-defect interaction profiling,[7] Raman spectroscopy,[8] etc. The most reliable quantitative technique for studying interstitials, particularly for Si, has been via the growth of interstitial clusters[9] or via the behavior of dopants known to diffuse by interstitial mechanisms.[10,11] In comparison, the quantitative study of vacancies in Si is even more difficult.[12] However, recently we have calibrated the Au labeling technique[13] and used it to make a number of quantitative measurements of V^{ex} generation in Si from high-energy ion (HEI) implantation.[14] In this work, we use the Au labeling technique to detect and quantitatively study the production of V-type defects near the front interface of a buried SiO_2 thin film in Si after implantation by 2 MeV $^{28}Si^+$. We also used the Monte Carlo simulation code TRIM (Ref. 15) to observe the nature of the excess defects at the buried Si/SiO_2 interface. Monte Carlo simulations also show that for structures of type Si/X, the mass of atoms in the thin-film X strongly influences the concentration of the excess defect (i.e., I or V type) at the front interface. The simulations suggest that not only the concentration but also the type of defect (I or V type) at the interface can be controlled by an appropriate choice of mass of the buried layer, affording a possible approach to control strain in overlayers.

a)Electronic mail: ramkik@wuphys.wustl.edu
b)Present address: Lawrence Livermore National Laboratory, Livermore, CA 94550.

0021-8979/2002/91(10)/6325/8/$19.00 © 2002 American Institute of Physics

Downloaded 30 Jul 2002 to 128.252.35.135. Redistribution subject to AIP license or copyright, see http://ojps.aip.org/japo/japcr.jsp

II. EXPERIMENT

The silicon-on-insulator (SOI) wafer used in this work had an approximately 1.5-μm-thick top Si layer, while the buried SiO_2 thin film was 0.2 μm thick. The thick Si top layer was prepared by rapid thermal chemical vapor deposition of a ~1.3-μm-thick Si layer on commercially available bonded SOI having a 0.2 μm silicon p/p^+ epi-Si top layer. The substrate below the buried oxide (BOX) was Czochralski silicon. The final 1.5±0.2-μm-thick Si was nominally undoped and the background O and C concentrations were below the SIMS detection limits of $\sim 5\times 10^{17}$ and $\sim 5\times 10^{16}$ cm^{-3}, respectively. Cross-sectional transmission electron microscopy (TEM) analysis of the as-grown wafer did not reveal any bulk or interfacial defects. The HEI implantation through the SiO_2 layer was achieved by implanting 2 MeV $^{28}Si^+$ in the dose range of $0.2-1\times 10^{16}$ cm^{-2} using a National Electrostatics Pelletron accelerator at an angle of 7° to the substrate normal. The beam current was 1.4 μA while the substrate temperature was held at 70 °C to prevent amorphization. Since the projected range (R_p) of the 2 MeV Si implant is ~2 μm with a straggle of ~0.25 μm [as calculated from TRIM98 (Ref. 16)] the interstitial-type defect is behind the SiO_2 layer.

Previously, V-type defects have been probed by a second Si implant of suitably chosen energy such that the R_p of this implant lies in the region of the vacancies.[13,17] A suitably chosen heat treatment then induces recombination between the vacancies and injected interstitials. Here, Si was implanted in the interface region of the 1×10^{16} cm^{-2} dose HEI sample with energies of 1.15 ($R_p \sim 1.41$ μm), 1.3 ($R_p \sim 1.52$ μm), or 1.5 MeV ($R_p \sim 1.66$ μm). The energy was varied slightly to compensate for any variation in the depth of the Si/SiO_2 interface as well as to control the number of Si atoms implanted near the interface. The areal density of the implanted Si atoms in the Si region near the interface was determined by measuring the position of the interface via RBS and then integrating the area up to the interface under the simulated implanted profile as determined by TRIM98. These samples were then annealed at 760 °C for 1020 s in a tube furnace under 1 atm of Ar (flow rate of 1.5 lpm). Depending upon the nature of the preexisting defects near the interface, this anneal will either grow interstitial clusters or recombine the added Si atoms with any existing V-type defects. The defect production in the SOI wafers was compared with bulk Si(100) wafers of float-zone type (FZ), where the identical 2 MeV Si implant in the dose range of $0.2-1\times 10^{16}$ cm^{-2} Si was carried out.

Finally, the vacancy defect profiles were measured using Au labeling[18] by implanting 68 keV $^{196}Au^+$ at a dose of 8×10^{14} cm^{-2} followed by a drive-in anneal at 750 °C (in 1 atm Ar with flow rate of 1.5 lpm). The anneal was performed until the saturation of Au in the V^{ex} region.[19] Rutherford backscattering using 2.8–3.0 MeV $^4He^{2+}$ was performed to measure the resulting Au profiles. Calibration experiments reported previously[13] have shown that under these HEI implant conditions the V^{ex} concentration is equal to the Au concentration multiplied by the calibration factor $k=1.2$.

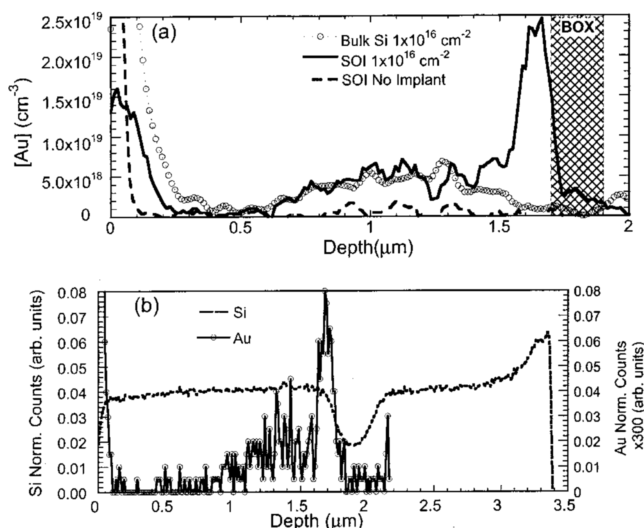

FIG. 1. (a) Experimentally observed Au profile after Au labeling for a SOI substrate (solid line) containing a high-energy implant (HEI) with 2 MeV Si at a dose of 1×10^{16} cm^{-2}. Also shown is the Au profile into a bulk Si wafer containing the identical HEI (open circles) and a SOI sample without the HEI (dashed line). The buried oxide layer (BOX) is indicated by the shaded area. (b) Overlaid signals of Au (open circles) and Si (dashed line) using the depth scales obtained via RBS. This overlay was used to determine that the rear edge of the extra Au peak in the SOI samples was at the front edge of the BOX layer.

The Monte Carlo binary collision code TRIM98 (Ref. 16) was also used to determine the nature of the excess defects at the interface following the implantation. A Si(1.5 μm)/SiO_2(0.2 μm)/Si structure was used to simulate damage production due to a 2 MeV ^{28}Si implant at an incident angle of 7°. The atomic densities used were 6.98×10^{22} atoms/cm^3 for SiO_2 and 4.98×10^{22} atoms/cm^3 for Si. The damage production was observed using a full damage cascade calculation. The displacement energy (E_d) used for the Si substrate and the buried layer in this and all subsequent TRIM calculations was 15 eV. Additional TRIM simulations were carried out to determine the dependence of the excess defects at the front interface on the mass of atoms in the buried thin film. The implant parameters were identical to the previous simulation. These additional simulations were carried out using the Si/X/Si heterostructure with the buried layer X of thickness 0.2 μm and density identical to SiO_2 of 6.98×10^{22} atoms/cm^3 but containing atoms of mass 12, 28, 31, and 73 amu. The depth of the thin film was 1 μm from the surface (as opposed to the earlier simulation where it was at a depth of 1.5 μm). Following the full cascade damage calculation, local recombination was used to determine the defect excess. In addition, the ballistic contribution to intermixing of the thin-film and substrate atoms was also followed.

III. RESULTS AND DISCUSSION

A. Excess defects at the buried Si/SiO_2 interface: Experimental findings

Figure 1(a) shows the typical Au profile obtained in a HEI sample with a 1×10^{16} cm^{-2} dose Si implant in the SOI substrate. Also shown is the Au labeling into a SOI substrate

Downloaded 30 Jul 2002 to 128.252.35.135. Redistribution subject to AIP license or copyright, see http://ojps.aip.org/japo/japcr.jsp

without any HEI. Three distinct regions of Au can be identified in Fig. 1(a) for the HEI samples: the surface implanted Au peak in the region of 0–0.2 μm, the Au profile in the window of 0.5–1.5 μm, and the peak in the region between 1.6 and 1.8μm. As compared to this, there is no Au trapped in the sample without any prior implant. The Au profile in the region of 0.5–1.5 μm is known to arise due the V^{ex} defects.[18] This region (referred to as the $V_{\mathrm{Si}}^{\mathrm{ex}}$ region) has been studied extensively in bulk float-zone Si.[14] We have recently shown[13] that for the dose conditions used in this work, the Au concentration in the $V_{\mathrm{Si}}^{\mathrm{ex}}$ region is related to the V^{ex} concentration by a calibration factor $k=1.2$. To determine if the profile in the SOI sample was quantitatively similar to that obtained in the bulk FZ-Si substrates, the profiles from a $1\times10^{16}\ \mathrm{cm}^{-2}$ dose HEI in SOI and bulk FZ Si were compared. As shown in Fig. 1(a), after Au drive-in into the as-implanted samples, a similar profile was obtained for both substrates in the region of 0.5 to ~1.5 μm. However, an essential difference between the Au profiles of the two substrates is the "extra" Au peak in the region between ~1.6 and 1.8 μm. To determine the precise position of this extra peak, the Au signal was overlaid with the Si substrate signal using the depth scales obtained via RBS.[20] As shown in Fig. 1(b), the rear edge of the Au peak corresponds to the front edge of the buried SiO_2 thin film, as indicated by the dip in the Si signal. This proved that the Au peak in the region between ~1.6 and 1.8 μm corresponded to Au at the front interface of the Si/SiO_2 layer.

To determine the nature of the defects that resulted in Au trapping in this interface region, extra Si atoms were added following the $1\times10^{16}\ \mathrm{cm}^{-2}$ dose HEI implant. The extra atoms were then reacted with the existing defects at the interface by a 760 °C and 1020 s implant. If interstitial defects are present at the interface, the extra Si atoms will tend to cluster with them and under the chosen anneal conditions would ripen to create large interstitial clusters of {311}-type defects.[21] These defects should show up as an increase in the concentration of trapped Au (Ref. 22) or be visible under TEM. On the other hand, if V-type defects are present at the interface, the extra Si atoms will recombine with some of the vacancies. This should lead to a decrease in the amount of Au trapped following Au labeling. Alternately, the extra atoms could rapidly recombine at the Si/SiO_2 interface, which is known to be a sink for interstitials,[23] thereby leaving the defects and therefore the amount of trapped Au unchanged. Shown in Fig. 2(a) are the simulated TRIM implantation profiles for the low-energy Si atoms with respect to the experimentally measured position of the buried oxide layer. Also shown is the experimental Au profile for the SOI sample containing the $1\times10^{16}\ \mathrm{cm}^{-2}$ Si HEI (and 760 °C, 1020 s anneal). In Fig. 2(b) the result of implanting the extra Si atoms, as measured by Au labeling, is shown. Clearly, the amount of trapped Au has decreased after the second implant, indicating that these defects are V type. The change in the Au concentration as a function of the implanted Si atoms is shown more clearly in Fig. 2(c). Here, the number of implanted Si atoms was estimated from the area under the curve between 1.3 μm up to the front interface of the Si/SiO_2 region at ~1.59 μm [Fig. 2(a)]. The integrated doses were

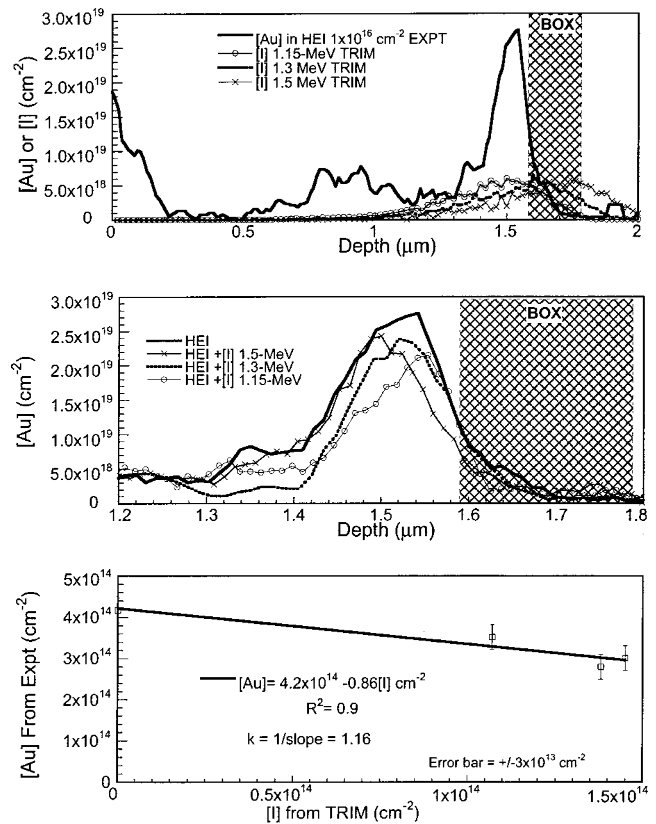

FIG. 2. (a) The experimentally observed Au profile for the 2 MeV, $1\times10^{16}\ \mathrm{cm}^{-2}$ Si HEI (solid line) in comparison with the spatial distribution of the interstitials obtained from TRIM calculations following the low-energy Si implants of 1.15–1.5 MeV. (b) Au profiles of the region near the buried interface following the interaction between the defects of the HEI and interstitials from the low-energy Si implants. (c) Integrated Au concentration after the various low-energy implants for the depth window of 1.3–1.59 μm plotted against the number of Si interstitials obtained from the TRIM calculations of (a) for the same depth window. The slope of the linear decrease on the amount of Au (~0.86) is identical to that obtained in the calibration experiment.

1.45×10^{14}, 1.38×10^{14}, and $1.07\times10^{14}\ \mathrm{cm}^{-2}$ for the 1.15, 1.3, and 1.5 MeV implants, respectively. The amount of trapped Au decreases linearly with the injected Si atoms. The slope of this variation, which gives the decrease in the number of Au atoms for every additional Si atom, is $\sim 0.86 \pm 0.26$. The reciprocal of this ratio, which measures the number of interstitials needed to reduce the amount of trapped Au by 1 atom is $\sim 1.16 \pm 0.35$. This number is in agreement with our earlier observed value of 1.2 ± 0.2 for $V_{\mathrm{Si}}^{\mathrm{ex}}$ in FZ Si, which measured the number of vacancies required to trap 1 Au atom. Furthermore, the amount of Si atoms placed at the interface (the areal density varied from 1.07×10^{14} to $\sim 1.45\times10^{14}\ \mathrm{cm}^{-2}$) is large enough to form interstitial clusters[21] when implanted alone. However, transmission electron microscopy observations in cross section did not show any extended interstitial defects at the interface in the HEI samples containing the second Si implant. Therefore, these three results: the linear decrease in the interface Au with Si injection, the agreement in the k value, and the absence of extended interstitial defects provides conclusive evidence that the existing defects at the interface (referred to as $V_{\mathrm{Int}}^{\mathrm{ex}}$) following the HEI are V type.

Downloaded 30 Jul 2002 to 128.252.35.135. Redistribution subject to AIP license or copyright, see http://ojps.aip.org/japo/japcr.jsp

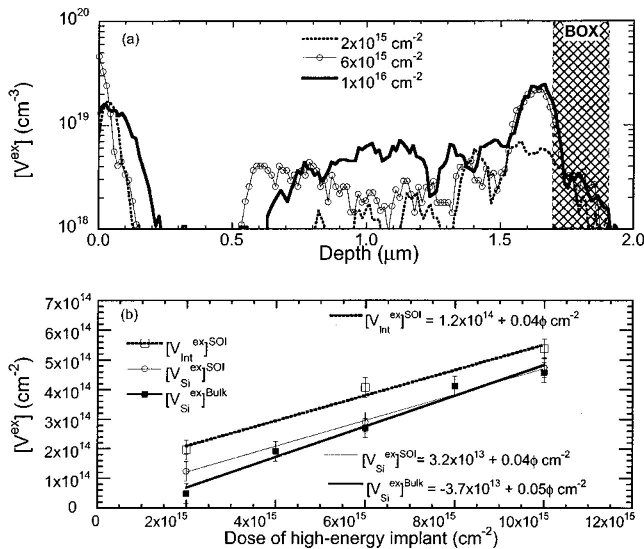

FIG. 3. (a) V^{ex} profile for various doses of the 2 MeV Si HEI obtained from Au labeling and calibration factor $k=1.2$. (b) Linear dose dependence was observed for the integrated (depth window of 0.5–1.5 μm) $[V_{Si}^{ex}]$ for the SOI (open circles) and bulk Si (solid squares). Also shown is the integrated $[V_{Int}^{ex}]$ (depth window of 1.5–1.8 μm) for the interface region (open squares), which also shows a linear increase with HEI dose.

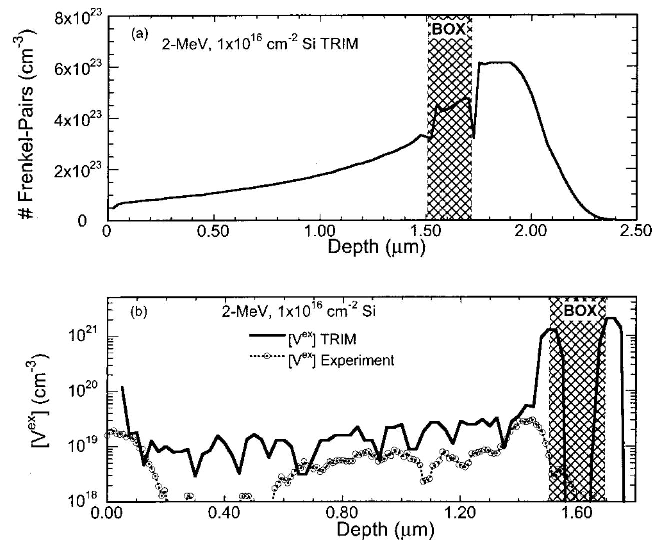

FIG. 4. (a) Frenkel pair profile obtained from the TRIM calculation for the 2 MeV, 1×10^{16} cm^{-2} Si HEI in the SOI substrate containing a 0.2-μm-thick BOX layer at a depth of 1.5 μm. (b) Excess vacancy defect profile following local recombination from the point defect distribution calculated from TRIM (solid line) compared to the experimentally observed V^{ex} profile for a 2 MeV, 1×10^{16} cm^{-2} Si HEI. The depth scale of the experimental profile was stretched by a factor of $\times1.15$ to align the buried interface position.

To further quantify the behavior of the V_{Int}^{ex}, a HEI dose-dependent study was performed. Shown in Fig. 3(a) is the V^{ex} profile for the SOI substrate as a function of HEI dose. Increasing dose increases V_{Si}^{ex} as well as V_{int}^{ex}. Using calibration factor k of 1.2 for the V_{Si}^{ex} and V_{int}^{ex} regions, the integrated V^{ex} concentration for the two regions as a function of the implanted Si dose can be plotted, as in Fig. 3(b). The depth window used to determine the areal concentration was 0.5–1.5 μm for V_{Si} and 1.5–1.8 μm for V_{Int}. Both regions show a linear increase with dose. Also shown in Fig. 3(b) is the V_{Si}^{ex} region observed for the bulk FZ Si. Clearly, the slopes of the V_{Si}^{ex} are within the error bars of these measurements (~15%). In addition, while the overall concentration of the V_{Int}^{ex} is greater the slope is similar to the V_{Si}^{ex} region. Thus, the V_{Int}^{ex} region behaves similar to the V_{Si}^{ex} region, suggesting that similar excess damage production mechanisms are operating for both cases.

B. Excess defects at the buried Si/SiO_2 interface: Simulation

Since binary collision codes have successfully predicted the existence of excess V-type defects in the V_{Si}^{ex} region,[24] we can use the Monte Carlo binary collision code TRIM to understand the effect of a buried thin film on the excess defect profile. Shown in Fig. 4(a) is the Frenkel pair profile produced following the 1×10^{16} cm^{-2} dose HEI in the SOI substrate. Following local recombination, the excess defect concentration is shown in Fig. 4(b), where the ordinate is in terms of the vacancy excess. The experimentally observed V^{ex} is also shown. Besides the excess in the V_{Si}^{ex} region from the surface to about 1.2 μm, there is also clearly a large V peak at the front interface. Therefore, the experimentally observed V_{int}^{ex} is qualitatively predicted by a simple binary collision calculation. The calculation of the excess as shown in Fig. 4(b) was based on the total number of atoms, i.e., both Si and O. As Fig. 5 shows, a significant concentration of O (peak concentration is $\sim4\times10^{18}$ cm^{-3}) is intermixed across the Si/SiO_2 interface. The areal density of O in the Si side of the interface is $\sim1.2\times10^{13}$ cm^{-2} for the 1×10^{16} cm^{-2} dose. This indicates that intermixed atoms could contribute significantly to the total atom concentration at the interface and will play a role in determining the behavior of the defects at the interface. In fact, we have recently reported on the thermal behavior of excess vacancies and the possible effect of O on their behavior.[25] Although the simulation predicts V_{int}^{ex}, a quantitative comparison between the experimentally observed V_{int}^{ex} and the TRIM observations shows that the simulation predicts values that are almost $10\times$ higher than

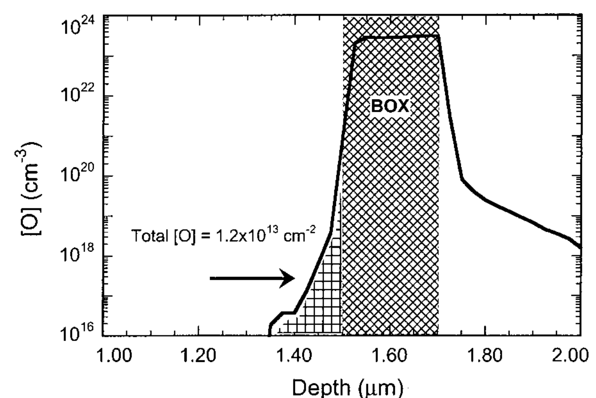

FIG. 5. Oxygen mixing profile following the TRIM calculation of a 2 MeV, 1×10^{16} cm^{-2} Si implant into the SOI substrate containing a 0.2-μm-thick BOX layer at a depth of 1.5 μm. The areal density of the intermixed oxygen was estimated for the dark shaded area, which corresponded to oxygen in the top Si layer.

Downloaded 30 Jul 2002 to 128.252.35.135. Redistribution subject to AIP license or copyright, see http://ojps.aip.org/japo/japcr.jsp

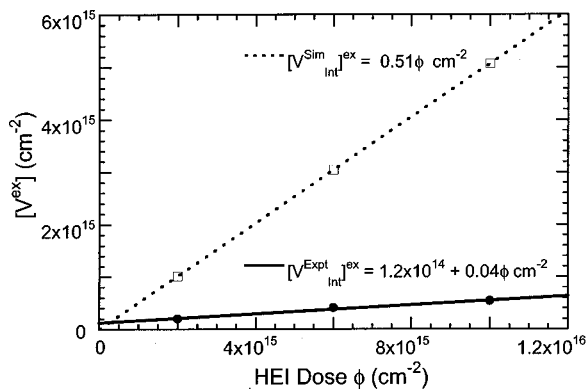

FIG. 6. Integral V^{ex}_{Int} as a function of the HEI dose obtained from the TRIM simulations (open squares) compared to the experimentally observed values (solid circles).

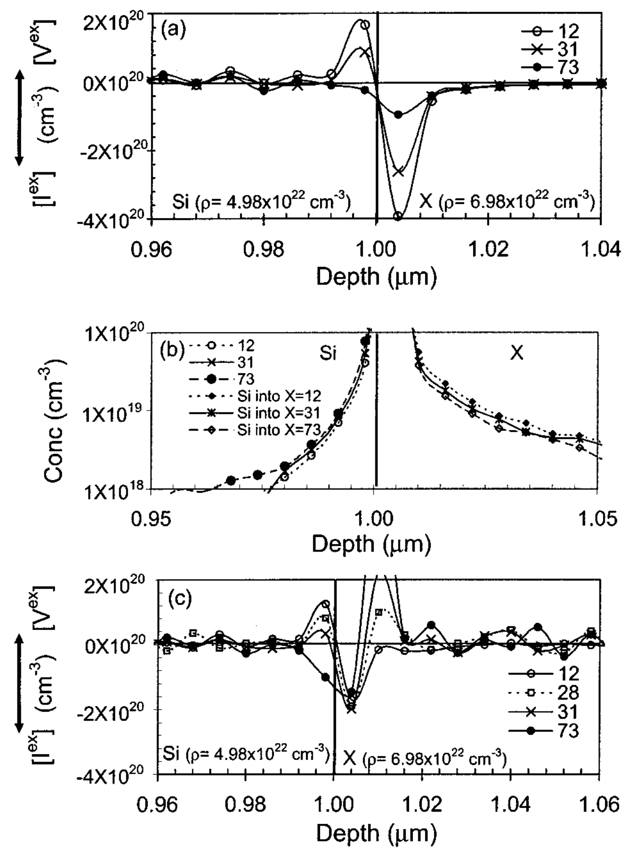

FIG. 7. (a) Simulated V^{ex} profiles at the frontside of the Si/X/Si structure as observed from TRIM simulations for various masses of X. The solid vertical line at 1 μm denotes the front interface between Si and X. The profiles here were estimated by treating any intermixed atoms from X to be interstitial type. All the simulations were for a 2 MeV, 2×10^{15} cm^{-2} Si HEI into a 1-μm-thick top Si layer and 0.2-μm-thick X layer. The X layer had an atomic density of 6.98×10^{22} cm^{-3}. (b) Simulated concentration of the X atoms intermixed into the Si side of the front interface and the Si atoms intermixed into the X side. (c) Simulated V^{ex} profiles at the front interface obtained by treating the intermixed X atoms as substitutional impurities.

that observed experimentally. Shown in Fig. 6 are the integral V^{ex}_{int} from experiment and simulation. V^{ex}_{int} is $\sim10\times$ higher for the TRIM calculation over experiment. It must be remembered that the TRIM simulation only involves local recombination of defects. In the experiment, the Au drive-in is carried out at 750 °C. Given the fact that point defects in Si are very mobile, the true V^{ex} concentration must also take into account any dynamic effects following the recombination. A more sophisticated simulation taking into account the mobility and thermal stability of the various defect clusters and their interaction with impurities and interfaces must be used to give an accurate quantitative picture of the V^{ex} generation. Nevertheless, the qualitative agreement obtained by using the simple binary collision code like TRIM allows a preliminary study of the effect of various implant and substrate parameters on excess defect production.

C. Excess defects at buried Si/*X*/Si structures: Simulation

Given the qualitative success of the Monte Carlo calculation in verifying the nature of the excess defects at the interface, the study of various aspects of the excess defect production on thin-film properties can be attempted. As described earlier, hypothetical 0.2-μm-wide thin films containing atoms of mass 12, 28, 31, and 73 amu were placed at a depth of 1.0 μm in these simulations. A 2 MeV, 2×10^{15} cm^{-2} dose Si implant was simulated and the resulting excess defect production was evaluated. Figure 7(a) shows the V^{ex} profiles in these TRIM calculations. The immediately apparent feature is the decrease in V^{ex} at the frontside of the interface (between 0.98 and 1.0 μm) as a function of increasing mass. In fact, for the case of mass 73 amu, the excess defect becomes interstitial type (I^{ex}), indicating a *crossover* in the sign of the defect (i.e., V^{ex} to I^{ex}) at some intermediate mass. Shown in Fig. 7(b) are the concentration profiles for impurity atoms intermixed into the Si side of the front interface and the Si atoms recoiled into the thin film. Here, the case for mass$=28$ amu is not plotted because the X atoms could not be distinguished from the substrate Si atoms. In the estimation of the excess, the behavior of these intermixed impurity atoms, i.e., their substitutional vs. interstitial (1) character must be accounted for. While the substitutional impurities will annihilate vacancies, the I-type impurities will not. In the case of Fig. 7(a), the impurity was assumed to be I type. If the impurities are considered substitutional, the result is a decrease in the V^{ex} and an increase in I^{ex}. Figure 7(c) shows the effect of substitutional impurities on the resulting excess defect profile. The case for X of mass $=28$ amu is also included as now the X atoms need not be distinguished from the substrate case. V^{ex} has now decreased for the 12 and 31 amu cases, while I^{ex} has increased for 73 amu. It should be emphasized here that the calculations were done for hypothetical layers having atomic density of 6.98×10^{22} cm^{-3}. Therefore, the result for $X=28$ amu, corresponding to Si atoms, shows an enhanced V^{ex} at the interface of the atomic density change. Similar calculations performed with $X=28$ but with the atomic density of Si did not show enhanced V^{ex}.

Figure 8 plots the integrated V^{ex} at the front interface (the integral window is $\sim$0.9–1.0 μm) with and without the substitutional impurity atoms as a function of the mass of the thin-film atoms. Significantly, V^{ex} decreases linearly with increasing mass, with the position of the *crossover* from V^{ex} to I^{ex} occurring at approximately 61 amu (for interstitial impu-

Downloaded 30 Jul 2002 to 128.252.35.135. Redistribution subject to AIP license or copyright, see http://ojps.aip.org/japo/japcr.jsp

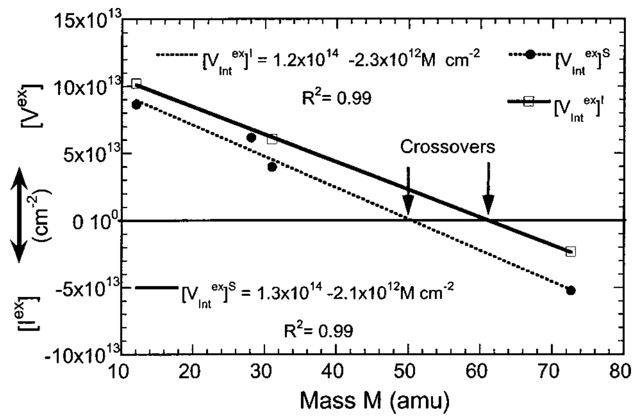

FIG. 8. Linear dependence of the $[V^{ex}_{Int}]$ on the mass of X atoms as obtained from TRIM simulations. The position of the crossover, which indicates the position of change in the sign of the excess defect at the front interface, is also marked. The position of the crossover varies depending on the behavior of the intermixed X atoms as interstitial or substitutional type. The crossover occurs at ~61 amu for interstitial-type X atoms, while it occurs at ~51 amu for substitutional type. The calculations here are for the 2 MeV, 2×10^{15} cm^{-2} Si implant into Si(1.5 μm)/X(0.2 μm)/Si heterostructure.

rities). For substitutional impurities, the *crossover* shifts to lower masses, and for this combination of Si implantation energy and depth of interface occurs at ~51 amu.

Table I lists the integral quantities of the Frenkel pair (FP) (I and V), the nuclear energy deposited, forward recoiled Si atoms, the impurity recoils, and the excess defects for the front interface. In general, there is a consistent variation in any quantity with increasing mass. For instance, the number of FPs in the Si substrate and the nuclear energy (E_d^{nuc}) deposited in the thin film increases with increasing mass, while the V^{ex} following the recombination of the FPs decreases. For the case when X is 28 or 31, the comparable FP density for 28 as compared to 31 arises because of the increased efficiency of energy transfer between two atoms of identical mass (i.e., here the implanted ion has mass 28 amu) as compared to between the different masses.[20] In addition, the number of impurity atoms intermixed into the frontside increases with mass, while the number of Si recoils in the thin film decreases with increasing mass for the depth window of 1.01–1.1 μm.

The net excess defect density following ion implantation through interfaces can be understood by considering the flux of atoms to various regions near the interfaces. For an elemental volume dV at a position P [Fig. 9(a)], the net rate of change in the number of atoms it contains is determined mainly by two factors; (i) the recoils from neighboring regions that stop in dV, and (ii) the atoms knocked out of dV by energetic collisions. We define a function $\rho(\acute{r})$, which is the rate per unit volume at which atoms from the neighboring regions are scattered by the ion-beam flux (including recoils, etc.) and come to rest in the volume element dV. The net flux to point P (into dV) is the integral of $\rho(\acute{r})$ over the surrounding regions, where $\rho(\acute{r})$ is nonzero, minus the rate at which atoms are kicked out of dV. In the homogeneous bulk, the net change in the number of atoms in dV is relatively small (the excess vacancies obtained experimentally are very small compared to the total point defect populations). However, if there is an inhomogeneity; i.e., a neighboring region where the recoil production rate is different

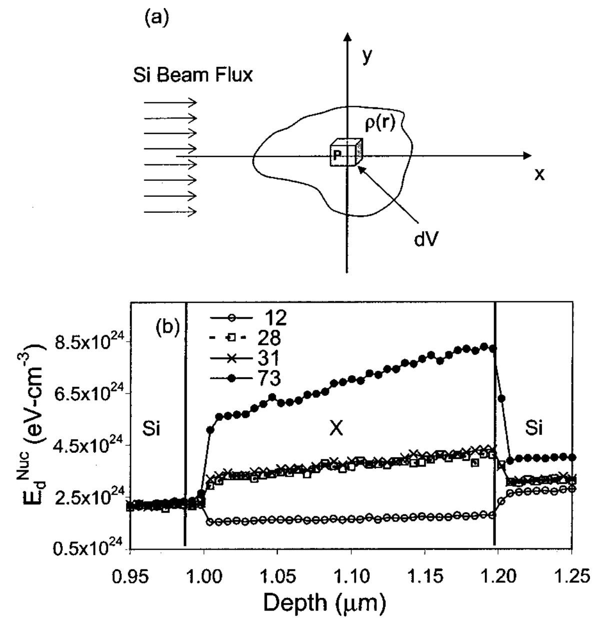

FIG. 9. (a) Net excess defect concentration following implantation in regions where the recoil production is changed over the bulk values can be estimated by the net flux of atoms into elemental volume dV from the surrounding regions. The function $\rho(\acute{r})$ determines the probability that an atom from a neighboring region will be knocked into dV. Thus, integration of $\rho(r)$ over the volume neighboring dV minus the number of atoms coming out from dV determines the net flux from which the net excess is determined. (b) TRIM calculation of the total energy deposited to nuclear stopping (E_d^{Nuc}) for the various X layers used. Change in E_d^{Nuc} in going from the bulk Si to the X layer provides one situation by which the recoil production in the X layer is different from bulk Si.

TABLE I. Results of the TRIM simulation for the 2 MeV, 2×10^{15} cm^{-2} Si implant into Si(1.0 μm)/X(0.2 μm)/Si heterostructure for the front Si/X interface. The excess defects are calculated in the Si side of the front interface in the depth window of 0.9–1.0 μm. The density of X for all the masses was $\sim 6.98 \times 10^{22}$ atoms/cm^3.

X atom Mass (amu)	No. of FPs (cm^{-2}) $<1.0\,\mu$m	E_d^{Nuc} (eV/ion) $<1.0\,\mu$m	Si recoils (cm^{-2}) $>1.0\,\mu$m	X recoils (cm^{-2}) $<1.0\,\mu$m	Excess defects (cm^{-2}) $+ve$ for V^{ex}/$-ve$ for I^{ex} Substitutional	Interstitial
12	3.1×10^{17}	6.3×10^{9}	8.3×10^{13}	1.6×10^{13}	8.6×10^{13}	1×10^{14}
28	3.3×10^{17}	1.2×10^{10}			6.2×10^{13}	
30	3.3×10^{17}	1.3×10^{10}	6.7×10^{13}	2.1×10^{13}	4×10^{13}	6×10^{13}
73	3.6×10^{17}	2.4×10^{10}	5.7×10^{13}	2.9×10^{13}	-5.3×10^{13}	-2.3×10^{13}

Downloaded 30 Jul 2002 to 128.252.35.135. Redistribution subject to AIP license or copyright, see http://ojps.aip.org/japo/japcr.jsp

from that in bulk Si, then another function $\rho^*(\acute{r})$ must be used in this region and the rate of accumulation of atoms in dV will be different from the bulk value. For instance, if P is close to a free surface, then $\rho^*(\acute{r})$ is zero beyond the surface, since the vacuum contributes nothing to the accumulation of atoms in dV. The rate of loss from dV is not affected by the presence of the surface, and therefore the approximate balance between the incoming and outgoing atoms in dV will be lost. In most cases where P is near a surface, net vacancies can be expected to accumulate in dV.

An effect that can cause a change in the recoil production rate near interfaces between different materials is the nuclear energy deposited into the material because of a different mass,[4] atomic density, etc., as compared to Si. From the simulations carried out here, the E_d^{Nuc} (in eV cm^{-3}) increases with increasing mass [Fig. 9(b)], as expected.[4] In addition, the E_d^{Nuc} changes rapidly in going across the interface. This leads to a change in recoil production across the interface and from our flux model provides a condition for an excess defect concentration that is enhanced over the bulk value. Further, the increasing E_d^{Nuc} will increase the cascade size (and the density of cascades) causing a ''spillover'' of mass and energy across the interface. This spillover is clearly manifested in the increase in the number of recoiled impurity atoms from the interface with increasing mass [Fig. 7(b)], and therefore changes the net flux in dV compared to the situation in bulk Si. These preliminary qualitative findings from the TRIM calculations emphasize that the mass of the interface atoms play an important role in the net excess defect population at the interface. Importantly, these simulations show that the defect type and/or defect density at the front interface can be controlled. While this model can be used to understand the presence of the V^{ex} peak at various interfaces, for instance, at the back SiO_2/Si interface [Fig. 4(b)], it does leaves out secondary effects, such as the reduction in the energetic particle flux with distance.

IV. CONCLUSION

The experiments reported here have clearly identified the nature of defects produced at a front interface of a buried thin film during irradiation of a heterostructure. Excess defects were created by a high-energy implant of 2 MeV Si into a SOI substrate containing Si(1.8 μm)/SiO_2 (0.2 μm)/Si. The Au labeling technique was then used to profile the excess defects. Besides Au trapping in the well-characterized excess vacancy-type defect region in the top Si region ($V_{\mathrm{Si}}^{\mathrm{ex}}$), additional Au trapping was observed at the frontside of the buried Si/SiO_2 interface. The nature of defects resulting in this trapping was investigated by additional low-energy Si implants. Following the low-energy Si implant and annealing at 760 °C for 1020 s, Au labeling showed a linear decrease in the amount of trapped Au with Si interstitial dose. The ratio of the number of Si atoms injected to the reduction in number of Au atoms trapped, k^{Int}, was $\sim 1.16 \pm 0.35$. TEM measurements did not show the presence of any extended interstitial-type defects. Therefore, the decrease in trapped Au with increasing number of low-energy Si atoms, the close correspondence of the k^{Int} to $k(1.2 \pm 0.2)$, and the lack of evidence of extended interstitial defects, clearly proved that the defects at the frontside of the buried interface were vacancy type. The concentration of the $V_{\mathrm{Int}}^{\mathrm{ex}}$ was found to increase linearly with increasing HEI dose with a slope similar to that of the $V_{\mathrm{Si}}^{\mathrm{ex}}$ suggesting that a similar damage production mechanism is involved at the interface.

Monte Carlo simulations of 2 MeV Si implantation into a Si(1.5)/SiO_2(0.2 μm)/Si heterostructure confirmed the existence of excess vacancy-type defects at the frontside of the buried interface. Further simulations were performed on structures of type Si(1.0 μm)/X(0.2 μm)/Si using 2 MeV Si, and varying the mass of X from that of 12–73 amu. The mass of X was found to be a very important parameter in the concentration of the excess defects at the front interface. A change in sign of the excess defect from V to I type at the front interface occurred for a mass of ~61 amu or greater, when the defects were treated as interstitial type. This transition shifted to lower mass (~51 amu) when the impurity atoms from the buried layer were treated as substitutional-type defects.

The experimental results and Monte Carlo simulations suggest that it may be possible to control the sign of the defect at buried interfaces. This may be an important effect considering the fact that point defects and their clusters at the interface can be used to tailor the strain of the overlayer. For instance, consider the presence of vacancy clusters near the front interface of a Si/X/Si heterostructure, wherein the top Si layer is sufficiently thin. In this case, a thin overlayer of Si can be subject to slightly larger compressive stresses, simply because of the additional available volume provided by the clusters. The sign of the applied stress can be reversed if instead of vacancies, an excess of interstitials existed at the interface. In other words, it is possible to envision tailoring the overlayer to accommodate an appropriate stress simply by choosing the right combination of the buried layer mass and implant parameter.

ACKNOWLEDGMENTS

The authors are indebted to Cliff King and George Celler for providing the SOI wafers. Many enlightening moments have been spent with members in the ''party room'' at Bell Laboratories and they will be missed. One of the authors (R. K.) also thanks Karl-Heinz Heinig for useful discussions. Research performed at Oak Ridge National Laboratory was sponsored in part by Oak Ridge Associated Universities under Contract No. DE-AC05-76OR00033 and by the U.S. Department of Energy, Office of Science, Laboratory Technology Research Division and the Division of Materials Sciences under Contract No. DE-AC05-00OR22725 with UT-Battelle, LLC.

[1] R. F. Wolffenbuttel, J. Micromech. Microeng. **6**, 138 (1996); K. Vanhollebeke, I. Moerman, P. Van Daele, and P. Demeester, Prog. Cryst. Growth Charact. Mater. **41**, 1 (2000).
[2] See review by U. Gösele and Q.-Y. Tong, Annu. Rev. Mater. Sci. **28**, 215 (1998).
[3] J. W. Mayer and S. S. Lau, in *Surface Modification and Alloying* (Plenum, New York, 1983); L. C. Feldman and J. W. Mayer, in *Fundamentals of Surface and Thin-Film Analysis*, North-Holland, NY (1986).
[4] M. Nastasi and J. W. Mayer, Mater. Sci. Eng., R. **R12**, 1 (1994).

Downloaded 30 Jul 2002 to 128.252.35.135. Redistribution subject to AIP license or copyright, see http://ojps.aip.org/japo/japcr.jsp

[5] A. Uedono, T. Kitano, M. Watanabe, T. Moriya, T. Kawano, S. Tanogawa, R. Suzuki, T. Ohdaira, and T. Mikado, Jpn. J. Appl. Phys., Part 1 **35**, 2000 (1996).
[6] R. A. Brown and J. S. Williams, J. Appl. Phys. **81**, 7681 (1997).
[7] M. Tamura, T. Ando, and K. Ohyu, Nucl. Instrum. Methods Phys. Res. B **59/60**, 572 (1991).
[8] M. B. Huang and I. V. Mitchell, J. Electron. Mater. **28**, 385 (1999).
[9] J. Y. Cheng, D. J. Eaglesham, D. C. Jacobson, P. A. Stolk, J. L. Benton, and J. M. Poate, J. Appl. Phys. **80**, 2105 (1996).
[10] D. J. Eaglesham, P. A. Stolk, H.-J. Gossmann, and J. M. Poate, Appl. Phys. Lett. **65**, 2305 (1994).
[11] H.-H. Vuong, H.-J. Gossmann, L. Pelaz, G. K. Celler, D. C. Jacobson, D. Barr, J. Hergenrother, D. Monroe, V. C. Venezia, C. S. Rafferty, S. J. Hillenius, J. McKinley, F. A. Stevie, and C. Granger, Appl. Phys. Lett. **75**, 1083 (1999).
[12] O. W. Holland, L. Xie, B. Nielsen, and D. S. Zhou, J. Electron. Mater. **25**, 99 (1996); S. L. Ellingboe and M. C. Ridgway, Nucl. Instrum. Methods Phys. Res. B **127/128**, 90 (1997); C. Szeles, B. Nielsen, P. Asoka-Kumar, K. G. Lynn, M. Anderle, T. P. Ma, and G. W. Rubloff, J. Appl. Phys. **76**, 3403 (1994).
[13] R. Kalyanaraman, T. E. Haynes, V. C. Venezia, D. C. Jacobson, H.-J. Gossmann, and C. S. Rafferty, Appl. Phys. Lett. **76**, 3379 (2000).
[14] R. Kalyanaraman, T. E. Haynes, D. C. Jacobson, H.-J. Gossmann, and C. S. Rafferty, Mater. Res. Soc. Symp. Proc. **610**, B9.4.1 (2000).
[15] J. P. Biersack and L. G. Haggmark, Nucl. Instrum. Methods **174**, 257 (1980).
[16] J. F. Ziegler, J. P. Biersack, and U. Littmark, *The Stopping and Ranges of Ions in Solids* (Pergamon, New York, 1985).
[17] R. Kalyanaraman, T. E. Haynes, V. C. Venezia, D. C. Jacobson, H.-J. Gossmann, and C. S. Rafferty, Mater. Res. Soc. Symp. Proc. **610**, B9.2.1 (2000).
[18] V. C. Venezia, T. E. Haynes, A. Agarwal, L. Pelaz, H.-J. Gossmann, D. C. Jacobson, and D. J. Eaglesham, Appl. Phys. Lett. **74**, 1299 (1999).
[19] The saturation time for the Au–V^{ex} trapping is found to depend upon the total V^{ex} concentration; R. Kalyanaraman, T. E. Haynes, O. W. Holland, and G. H. Gilmer, J. Appl. Phys. (submitted).
[20] See, for instance, W.-K. Chu, J. W. Mayer, and M.-A. Nicolet, *Backscattering Spectrometry* (Academic, Orlando, FL, 1978).
[21] D. J. Eaglesham, P. A. Stolk, H.-J. Gossmann, T. E. Haynes, and J. M. Poate, Nucl. Instrum. Methods Phys. Res. B **106**, 191 (1995).
[22] J. Wong-Leung, E. Nygren, and J. S. Williams, Appl. Phys. Lett. **67**, 416 (1995).
[23] D. Tsoukalas, C. Tsamis, and J. Stomenos, Appl. Phys. Lett. **63**, 3167 (1983).
[24] A. M. Mazzone, Phys. Status Solidi A **95**, 149 (1986); K. B. Winterbon, Radiat. Eff. **46**, 181 (1980).
[25] R. Kalyanaraman, T. E. Haynes, O. W. Holland, H.-J. L. Gossmann, C. S. Rafferty, and G. H. Gilmer, Appl. Phys. Lett. **79**, 1983 (2001).

Downloaded 30 Jul 2002 to 128.252.35.135. Redistribution subject to AIP license or copyright, see http://ojps.aip.org/japo/japcr.jsp